

## MICROSTRUCTURE AND WEAR RESISTANCE OF AN ARC-SPRAYED Fe-BASED COATING AFTER SURFACE REMELTING TREATMENT

H. L. Tian,<sup>a,b,1</sup> S. C. Wei,<sup>b</sup> Y. X. Chen,<sup>b</sup> H. Tong,<sup>b</sup>  
Y. Liu,<sup>b</sup> and B. S. Xu<sup>b</sup>

UDC 539.4

*The aim of the study was to improve the lamellar structure and wear resistance of arc-sprayed coatings. FeNiCrAl arc-sprayed coatings were remelted by the tungsten inert gas welding method. The as-sprayed and remelted specimens were subjected to comparative structural phase composition examination using optical microscopy, scanning electron microscopy and X-ray diffraction. Additionally, the effect of the remelting treatment on the wear mechanism of the arc sprayed coatings was also studied. It was found from the experiments that the tungsten inert gas surface process has the potential to form pore- and crack-free coatings. Further investigations showed that the dominant mechanism of wear for the as-sprayed coatings was oxide delamination and for the tungsten inert gas remelted coatings was cutting and ploughing.*

**Keywords:** high velocity arc spraying, remelting process, microstructure, wear.

**Introduction.** The arc spraying process is widely used to prepare different thin coatings, which is extensively applied in maintaining and rebuilding fields [1]. However, the coatings obtained with this process exhibit lamellar microstructure, high porosity, and low surface hardness, and their wear resistance is not sufficient for many applications [2]. Therefore, surface remelting treatment needs to be carried out to reinforce the adhesive strength and enhance the wear resistance of as-sprayed coatings.

The reduction in microinclusion content of coatings by surface melting using such processes as laser [3], plasma [4], and tungsten inert gas (TIG) [5] welding has been shown to improve coating toughness owing to the changes in their microstructure, chemical composition, and oxygen content. In recent years, several studies have been performed using the TIG method [6]. The process increases surface hardness, improves wear resistance, and results in little or no distortion. In this study, the microstructural properties, hardness, phase composition and wear resistance of Fe-based remelted coatings were ensured with a TIG torch.

**Experimental Method.** Fe–Ni–Cr–Al cored wire with a diameter of 2 mm was used to produce as-sprayed coatings. The chemical composition of the arc spraying wire was (wt.%): Ni < 10, Cr < 5, Al < 5, B < 1, Nb < 1, Re < 1, Fe – balance.

The wires were sprayed onto a grit blasted and degreased AISI 1045 steel substrate with dimensions of 100 × 100 × 10 mm using a self-designed HAS-02 wire arc gun system. The process parameters were optimized as follows: spraying voltage 28 V, spraying current 160 A, compressed air pressure 0.7 MPa, standoff distance, 200 mm. The thickness of the as-sprayed coatings was 400–500 μm and they were subsequently melted using a TIG torch. The TIG torch/arc was produced with an operating current ranging from 80 to 100 A. The remelting process was carried out at 3 and 4 mm/s speed and the electrode distance from the substrate surface varied between 3 and 5 mm. The shield gas flow (argon) was 12 l/min.

---

<sup>a</sup>School of Materials Science and Engineering, Beijing University of Aeronautics and Astronautics, Beijing, China (haoliangtian@163.com). <sup>b</sup>National Key Laboratory for Remanufacturing, Academy of Armored Forces Engineering, Beijing, China. Translated from Problemy Prochnosti, No. 2, pp. 90 – 97, March – April, 2014. Original article submitted November 22, 2013.

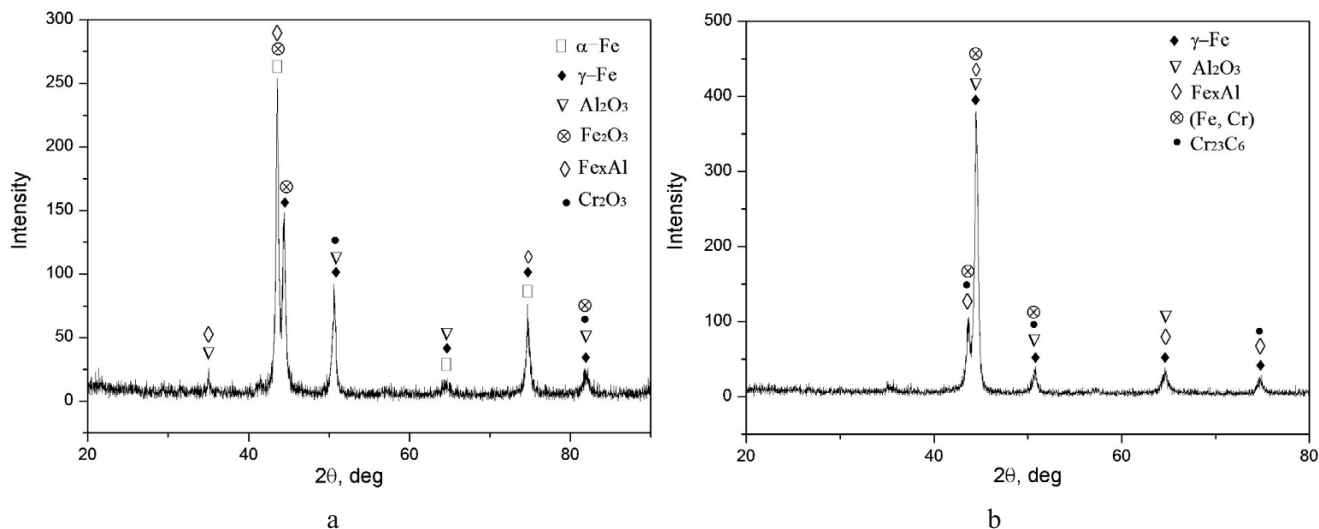


Fig. 1. XRD results for as-sprayed (a) and remelted (b) coatings.

The microstructure and chemical compositions of cross sections of as-sprayed and remelted specimens were compared using optical microscopy, scanning electron microscopy (SEM) and energy dispersive spectroscopy (EDS). X-ray diffraction (XRD) analysis was conducted to determine the phases formed in the alloyed surface layer.

Dry sliding wear tests were carried out using a ball-on-plate reciprocating machine at room temperature (25°C). The counterpart ball was quenched before the wear test. The abrading ball was a GCr15 ball with 65 HRC and of 4 mm in diameter. The applied load and sliding distance were 50 N and 2700 mm (with an increment of 3 mm), respectively. The sliding velocity was 3 mm/s. Five specimens were measured for each set of test parameters. The friction coefficient was monitored with a computer. The microstructure of worn surfaces and wear debris was analyzed by SEM to understand the wear mechanism for coated and uncoated specimens.

### Results and Discussion.

**X-Ray Diffraction.** X-ray diffraction analysis was performed on the surface of the as-sprayed and remelted coatings. The diffraction patterns are shown in Fig. 1a and 1b, respectively. As can be seen from Fig. 1a, α-Fe, γ-Fe and Fe–Al intermetallic compounds are major phases present at the surface of an as-sprayed coating. Moreover, during spraying, molten liquid drops are exposed to air and are oxidized in flight to the substrate, and many oxides, such as Al<sub>2</sub>O<sub>3</sub>, Cr<sub>2</sub>O<sub>3</sub>, and Fe<sub>3</sub>O<sub>4</sub>, can be present at the exposed surfaces of splats prior to the deposition of the subsequent layer [7].

Figure 1b shows the phases of a remelted coating. These are mainly γ-Fe, Fe–Al intermetallic compounds, a (Fe, Cr) solid solution, and Cr<sub>23</sub>C<sub>6</sub> carbides, and weak peaks are assigned to Al<sub>2</sub>O<sub>3</sub> oxides. These results clearly confirm that the elements Fe, Cr, Ni, and Al dissolved in the coating matrix then formed more alloy phases, while few oxides were detected in the coating after the TIG remelting process.

**Microstructural Examination.** A comparison was made of the cross-sectional micrographs of a remelted coating formed by TIG (Fig. 2b) and an as-sprayed coating (Fig. 2a). A thin white layer is observed at the interface in Fig. 2b, which indicates a good metallurgical bonding between the remelted coating and the substrate.

In the bonding zone, an extremely high rate of heat transfer occurred between the molten pool and the substrate and a large melt was obtained on cooling leading to a very high rate of solidification [8]. The solid/liquid interface grew in a flat form giving rise to the formation of a bright flat grain in the coating as shown in Fig. 2b.

Figure 3a shows a cross-sectional SEM image of an as-sprayed coating before TIG treatment. Laminated structures with many pores and cracks arise in the lamellar structure and the interface between the coating and substrate. Figure 3b shows the cross-sectional morphology of a remelted coating. In contrast to Fig. 3a, the remelted coating was characterized by a more uniform structure, the absence of structure lamination, and decreased surface roughness and porosity. In order to analyze porosity quantitatively, a computer image analyzer was employed. It was

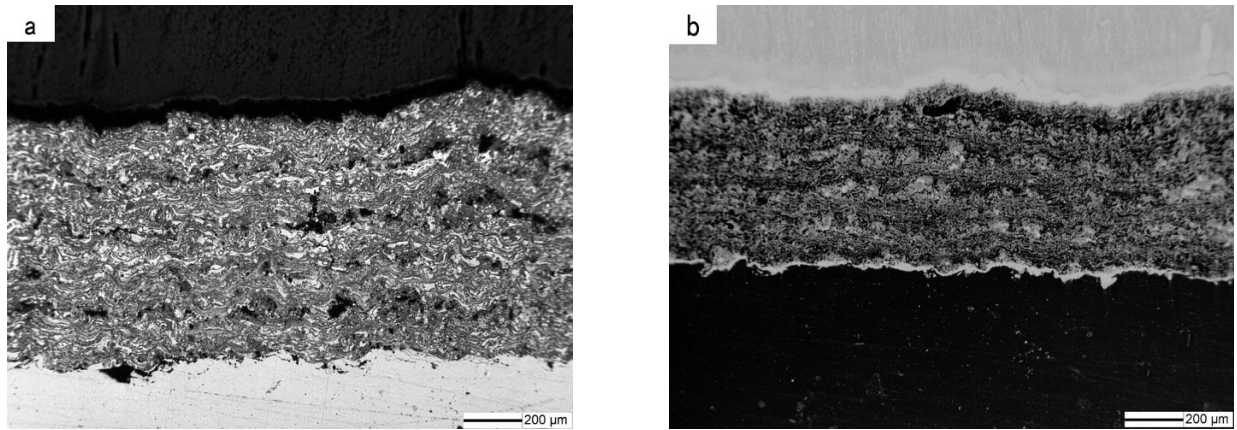


Fig. 2. Optical micrographs of cross sections of as-sprayed (a) and remelted (b) coatings.

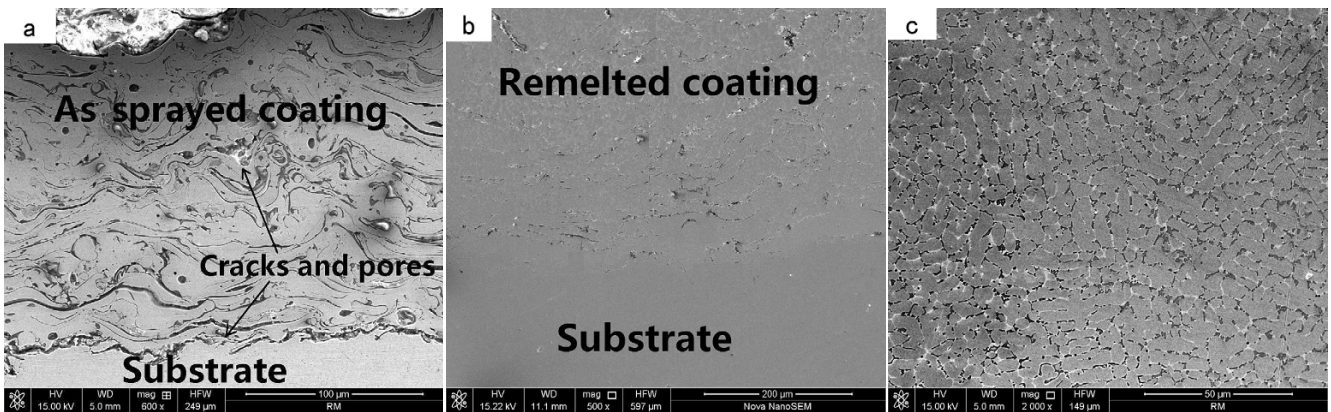


Fig. 3. SEM cross-sectional morphology of as-sprayed (a) and remelted (b) coatings and high magnification morphology (c).

observed that porosity of as-sprayed coatings was 17–22% and remelted coatings show a dramatically reduced porosity of only 1.1–2.8%.

A typical pattern of higher magnification morphology observed for remelted coatings is shown in Fig. 3c. The SEM investigations revealed a distinct refinement of the structure. Microcracks delaminating the remelted coating were not observed. Depending on the material cooling rate function of the adopted treatment parameters, different morphology phases were observed, among them microdendrite and cellular–dendrite ones were predominant.

**Microhardness Investigations.** The microhardness profiles of as-sprayed and remelted coatings with a coating depth are shown in Fig. 4. It can be seen that the microhardness of the as-sprayed coating gradually increased with the distance from the substrate to the coating surface. The hardness of the as-sprayed coating was about 480–580 HV0.1. The anisotropy of the coating, resulting from the characteristic layered structure of an as-sprayed material, was responsible for the microhardness values and their distribution.

The hardness increased to about 670–740 HV0.1 for the as-sprayed coating after remelting treatment. This result confirms that there are marked differences in the microstructures of the coatings before and after the TIG remelting process. The remelted coating exhibits high hardness corresponding to such hard phases, as intermetallic compounds and a (Fe, Cr) solid solution distributed in the dense structure, possessing homogeneous chemical dispersion and adequate recrystallization.

**Wear Resistance Performance.** The variation of friction coefficient for the substrate, as-sprayed coating, and TIG remelted coating are compared in Fig. 5. The average friction coefficient values of the substrate, as-sprayed coating and remelted coating were calculated as 0.9, 0.6, and 0.5, respectively. It can be seen that the TIG remelted

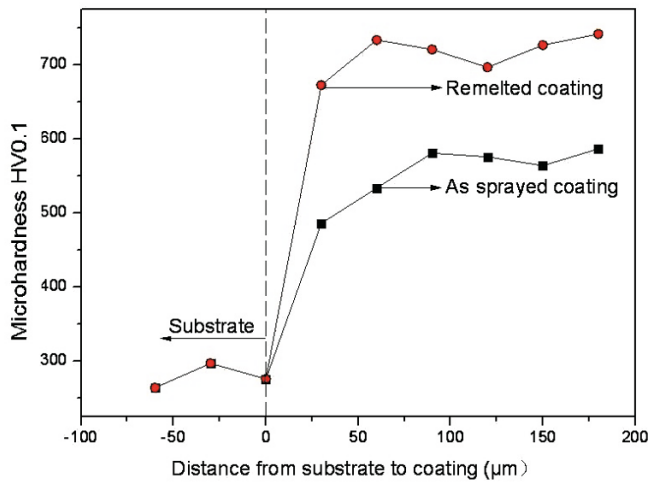


Fig. 4

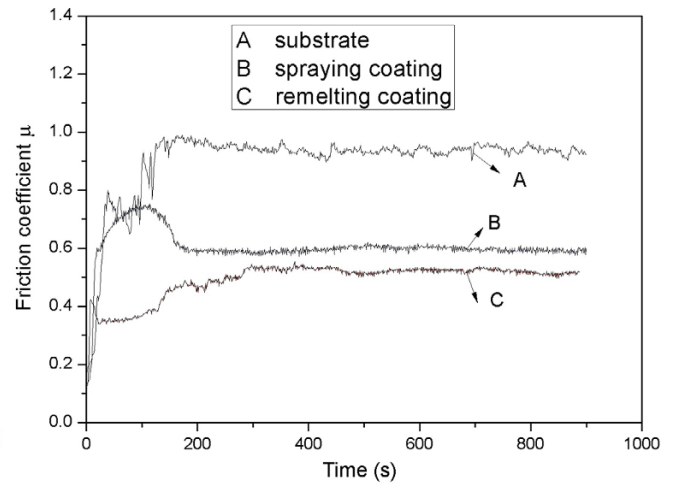


Fig. 5

Fig. 4. Microhardness of as-sprayed and remelted coatings.

Fig. 5. Friction coefficients of Fe-based coatings and a substrate.

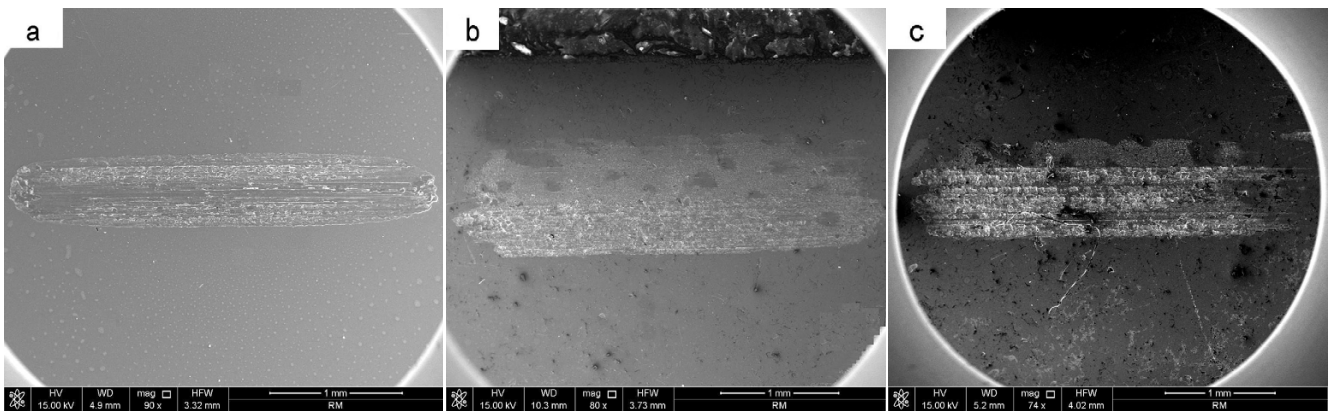


Fig. 6. Macrographs of wear tracks of the substrate (a), as-sprayed (b) and remelted (c) coatings.

coating is more effective in improving wear resistance, and its friction coefficient curve shows a smooth variation. The friction coefficient curve for the remelted coating is more stable than that of the substrate with a sliding distance.

In order to compare the wear resistance of an as-sprayed coating and remelted one, SEM examination of the worn surfaces was undertaken, as shown in Fig. 6. It can be seen that the wear track of the remelted coating (Fig. 6c) is shallower than those of the as-sprayed coating (Fig. 6b) and the substrate (Fig. 6a). The wear volume losses for the substrate, as-sprayed coating and remelted coating were measured as  $3.78 \cdot 10^{-6}$ ,  $2.46 \cdot 10^{-6}$ , and  $1.13 \cdot 10^{-6} \mu\text{m}^3$ , respectively, revealing that the TIG remelted coating has the lowest wear volume for the dense microstructure. A fine cellular structure was formed after the TIG remelting process.

For understanding the wear mechanisms of as-sprayed and remelted coatings, SEM and EDS analysis of the wear surface and wear debris was undertaken, as shown in Figs. 7 and 8, respectively. The EDS examination of the wear tracks of the as-sprayed coating confirmed that the chemical composition of the microzone of the wear surface is mainly 68.38 wt.% Fe, 9.28 wt.% Al, 21.13 wt.% O, and 1.21 wt.% Nb (Fig. 7b). The results reveal the presence of iron oxides practically on all the surfaces of the coatings that were tested (Fig. 7a). The concentration of these oxides fell as the sliding distance increased. This can be explained by the low cohesive strength among splats, numerous pores and microcracks already present in the as-sprayed coating or generated during the tests carried out. Under the dry sliding conditions, the induced strong shearing stress initiates microcracks, which, together with inherent

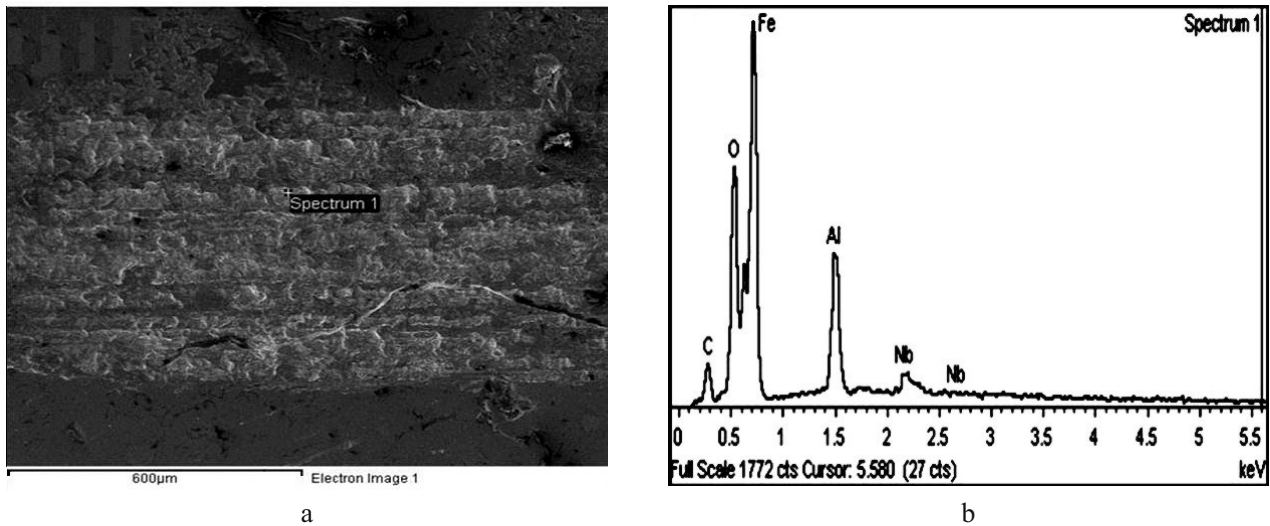


Fig. 7. SEM and EDS analysis of an as-sprayed coating: (a) SEM morphology of the wear track; (b) EDS analysis of the wear track.

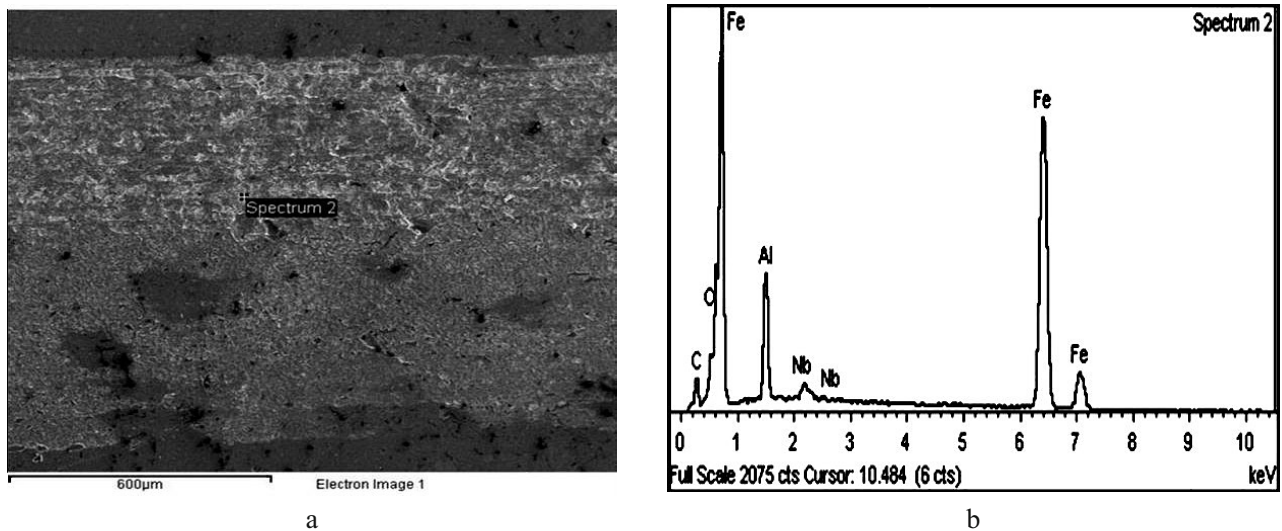


Fig. 8. SEM and EDS analysis of the remelted coating: (a) SEM morphology of the wear track; (b) EDS analysis of the wear track.

microcracks, grow and extend along the boundaries of the splats. When the stress intensity is close to the fracture toughness of the coating, complete splats should break off from the coating [9].

The wear surface of the remelted coating is distinguished by discontinuous parallel grooves (see marked spectrum 2 in Fig. 8a), which are formed as the hard abrasive phases penetrating into the worn coating surface and then ploughing the matrix material from the groove to the side. This causes the so-called grooving wear mode [10]. Therefore, cutting and ploughing are the main abrasive wear mechanisms. But, the distribution of a (Fe, Cr) solid solution and  $\text{Cr}_{23}\text{C}_6$  hard phases surrounded by the matrix of  $\gamma\text{-Fe}$  will be of benefit for improving the wear resistance. The surrounding ductile structure ( $\gamma\text{-Fe}$ ) will absorb energy, while the coating bears a high load, releasing residual stresses [11]. This structural characteristic of abrasive particles embedded in the ductile matrix will eliminate the microcracks from initiation along the oxide boundaries under the action of concentrated stresses and improve the wear resistance of the remelted coating. Furthermore, oxygen atoms were not detected in the wear surface (Fig. 8b), which confirms that the remelted coating has the ability to resist oxidation wear failure. A very dense microstructure

and low porosity characteristics also prevent the abrasive particles from microcutting the surface by breaking them up and causing them to lose their cutting function [12]. Therefore, the coating has excellent abrasive wear resistance.

## CONCLUSIONS

1. Coatings produced by TIG remelting of Fe-based alloy coatings are free from pores and cracks and show good metallurgical bonding with the substrate. The primary phases of the remelted coating were identified as  $\text{Cr}_{23}\text{C}_6$  carbides and a Fe-based solid solution.

2. The consequence of remelting treatment is the transformation  $\alpha\text{-Fe} \rightarrow \gamma\text{-Fe}$ . The wear resistance of coated specimens is far better than that of uncoated ones. Particles as thin flakes combined with energy dispersive spectroscopic analysis confirm that oxide delamination is the dominant wear mechanism of an as-sprayed coating. Cutting and ploughing are the main abrasive wear mechanisms of the remelted coating.

**Acknowledgments.** The authors are grateful for the support provided by 973 Project (2011CB013403), and the Natural Science Foundation of China (51105377, 50971132), National Science and Technology Supporting Project (No. 2011baf11B07).

## REFERENCES

1. Y. X. Chen, X. B. Liang, Y. Liu, et al., "Effect of heat treatment on microstructure and residual stress of wire arc sprayed high carbon steel coating," *Surf. Eng.*, **26**, 407–412 (2010).
2. S. Buytoz and M. Ulutan, "In situ synthesis of SiC reinforced MMC surface on AISI 304 stainless steel by TIG surface alloying," *Surf. Coat. Technol.*, **200**, 3698–3704 (2006).
3. N. Ahmed, M. S. Bakare, D. G. McCartney, and K. T. Voisey, "The effects of microstructural features on the performance gap in corrosion resistance between bulk and HVOF sprayed Inconel 625," *Surf. Coat. Technol.*, **204**, 2294–2301 (2010).
4. T. T. Wong, G. Y. Liang, G. An, and J. M. K. MacAlpine, "The electrical conductivity of laser-remelted and plasma-sprayed Ni and Cr coatings," *J. Mater. Process. Technol.*, **159**, 265–271 (2005).
5. B. Arivazhagan, S. Sundaresan, and M. Kamaraj, "Effect of TIG arc surface melting process on weld metal toughness of modified 9Cr–1Mo (P91) steel," *Mater. Lett.*, **62**, 2817–2820 (2008).
6. Y. Shi, H. Zhang, and S. Y. Liu, "Laser fine cladding on miniature thin wall parts," *Surf. Eng.*, **27**, 464–469 (2011).
7. J. Morimoto, Y. Sasaki, and S. Fukuhara, "Surface modification of  $\text{Cr}_3\text{C}_2\text{-NiCr}$  cermet coatings by direct diode laser," *Vacuum*, **80**, 1400–1405 (2006).
8. G. Azimia and M. Shamanianb, "Effects of silicon content on the microstructure and corrosion behavior of Fe–Cr–C hardfacing alloys," *J. Alloys Compd.*, **505**, 598–603 (2010).
9. Y. X. Chen, B. S. Xu, and Y. Liu, "Structure and sliding wear behavior of 321 stainless steel/Al composite coating deposited by high velocity arc spraying technique," *Trans. Nonferrous Met. Soc. China*, **18**, 603–609 (2008).
10. J. B. Cheng, X. B. Liang, and B. S. Xu, "Formation and properties of Fe-based amorphous/nanocrystalline alloy coating prepared by wire arc spraying process," *J. Non-Cryst. Solids*, **355**, 1673–1678 (2009).
11. M. Vite, M. Castillo, and L. H. Hernandez, "Dry and wet abrasive resistance of Inconel 60 and stellite," *Wear*, **258**, 70–76 (2005).
12. J. M. Miguel, J. M. Guilemany, and S. Vizcaino, "Tribological study of NiCrBSi coating obtained by different processes," *Tribol. Int.*, **36**, 181–187 (2003).